

## Thermal transport properties in aluminum crystals at liquid-helium temperature

Constantin Papastaikoudis

*Nuclear Research Center "Dimocritos" Aghia Paraskevi, Athens, Attiki, Greece*

Wilto Kesternich

*Institut für Festkörperforschung der Kernforschungsanlage Jülich, D-517 Jülich, Germany*

(Received 18 July 1977)

The orientation and magnetic-field dependence of the thermoelectric power and Ettingshausen-Nernst effect at liquid-helium temperatures in transverse magnetic fields up to about 50 kG, have been investigated in different single crystals of aluminum with the heat current in the [100], [110], [111], and [112] directions. The rotation diagram of the thermopower show anisotropies which agree with magnetoresistance measurements. On these anisotropies are superimposed the same characteristic peaks which appear in the magnetoresistance. These peaks are attributed to magnetic breakdown. The field dependence of the thermopower and of the Ettingshausen-Nernst voltage show large-amplitude sinusoidal oscillations when the magnetic field  $\vec{H}$  is parallel to the [001] direction. The oscillations are periodic in  $1/H$  and are due to networks of open and closed orbits extending over second- and third-zone Fermi-surface sheets.

### I. INTRODUCTION

In a previous paper, we reported the first observation<sup>1</sup> of giant oscillations in the thermopower of aluminum in a transverse magnetic field. The existence of these oscillations was also discovered independently by Thaler and Bass,<sup>2</sup> and by Sirota *et al.*<sup>3</sup> It was found that the thermopower oscillates with a period of  $\Delta(1/H) = 2.12 \times 10^{-6} \text{ G}^{-1}$  and that the amplitude of these oscillations increases nearly exponentially with inverse magnetic field. We attributed these oscillations to magnetic breakdown between the  $\beta$  orbits in the third zone of the Fermi surface and the adjoining orbits in the second zone, near the corners  $W$  of the Brillouin zone.

In the present paper, we attempt an extended investigation of the variation of the thermopower and the Ettingshausen-Nernst voltage as a function of the orientation of different samples in a transverse magnetic field and the magnitude of the field, for the purpose of performing a detailed study of magnetic breakdown to be compared with results from magnetoresistance.<sup>4</sup>

### II. EXPERIMENTAL DETAILS

Our experimental setup was originally not intended to perform thermoelectric measurements. The specimen holder and magnet are immersed in the same bath of liquid helium to allow galvanomagnetic measurements at the boiling temperature of helium under atmospheric or lower pressure. The attachment of a carbon resistor as a heater to the specimen (CR in Fig. 1) allowed for the creation of a temperature gradient along the specimen axis, thus allowing for thermomagnetic measurements with the possibility of measuring both the

dependence on rotation angle and oscillatory effects, but with the limitation that the absolute value of the thermovoltage and the oscillatory amplitudes could only be determined within an accuracy of about a factor of 2. The value of the temperature gradient and that of the absolute thermopower were obtained from measurements of the resistivity as a function of temperature  $\rho(T)$  in the following way. Between the potential leads 1-3, 3-2, and 1-2 (Fig. 1) the differential resistivity  $\rho_{13}(T_{13}) - \rho_{13}(4.2 \text{ K})$ ,  $\rho_{32}(T_{32}) - \rho_{32}(4.2 \text{ K})$ , and  $\rho_{12}(T_{12}) - \rho_{12}(4.2 \text{ K})$ , respectively, was measured and compared with the experimental temperature dependence  $\rho(T) - \rho(4.2 \text{ K})$  for aluminum.<sup>5</sup> This yields the three values  $T_{13}$ ,  $T_{32}$ , and  $T_{12}$ . These values are average temperatures between the corresponding potential leads, where the averaging depends on the variation of temperature along the sample. Assuming this variation to be an exponential decrease with distance from the heater, a value of  $\Delta T = T_2 - T_1 = 0.8 \text{ K}$  temperature gradient between contact 1 and 2 has been calculated for our experimental conditions. Due to the finite length

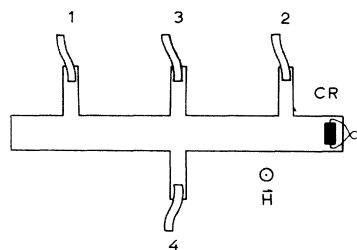


FIG. 1. Specimen shape and arrangement of potential leads. The heater CR is a carbon resistor.

of the sample and due to the potential leads as additional heat sinks, considerable deviations from the assumed exponential temperature dependence may occur, so that we must allow for a corresponding uncertainty:  $\Delta T = 0.8 \pm 0.3$  K.

The samples used in this investigation were prepared from different cylindrical single crystal blocks. After orientation by the Laue diffraction method, disks of about 1-mm thickness were cut from blocks. By spark machine polishing, the macroscopic surface roughness was removed and the surfaces of the disk were made parallel. The samples were etched for 1 min at 80°C in Pickling acid (0.25 H<sub>2</sub>SO<sub>4</sub>, 0.05 HNO<sub>3</sub>, 0.75 H<sub>3</sub>PO<sub>4</sub>), whereby the disk thicknesses were reduced by about 100 μm. When the required thickness was reached, the orientation was again determined by x rays. Then the sample shape was punched out of the disks, suitably oriented for the desired crystallographic direction of the temperature gradient. The final shape of the specimens is shown in Fig. 1. Their residual resistivity ratios (RRR) lay between 4000 and 7000.

The specimen could be rotated freely about its axis in a magnetic field, which was provided by a locally constructed Helmholtz superconducting coil, which had maximal intensity of about 50 kG. The output voltage signal was amplified by a galvanometer (Sefram, France) and recorded by an X-Y recorder or whenever higher accuracy was required (up to ±1 nV), by an integrating voltmeter (Solatron). The electrical connections to the potential leads were made by spring-loaded contacts.

### III. RESULTS

#### A. (100) rotation plane

The rotation diagram of the thermopower with  $\nabla T$  parallel to the [100] direction in a constant magnetic field  $H = 46$  kG and at 4.2 K is shown in Fig. 2. Two maxima with narrow double peaks occur, located symmetrically about the  $\vec{H} \parallel [001]$  direction. The heights of these peaks are approximately identical and the distances between them amount to 4°. These are the predominant features of the rotation diagram. They are comparable to the magnetic breakdown effects which were observed in the magnetoresistance<sup>4</sup> for the same crystal orientation of the specimen. The peaks are as high as 5–6 μV/K which may be compared to low-temperature thermovoltages without field<sup>6,7</sup> and also to the magnetothermopower in the absence of magnetic breakdown<sup>8,9</sup> in aluminum, which are always smaller by two orders of magnitude. The average thermopower outside of the peak regions in Fig. 2 is displaced from zero by

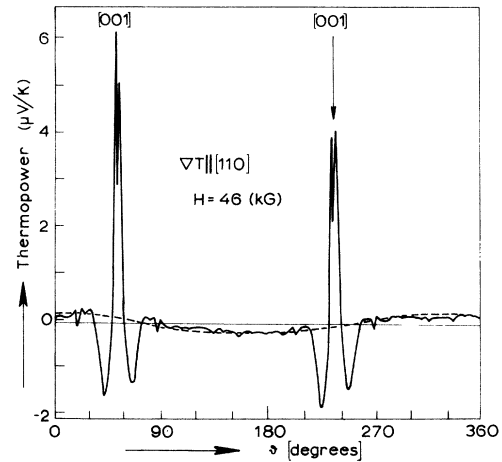


FIG. 2. Rotation diagram of the transverse magnetothermopower for  $\nabla T$  parallel to [110] and  $H = 46$  kG. Values of  $S$  are only accurate within ±40% (see experimental details).

about  $-0.05$  μV/K. This is the normal contribution of magnetothermopower. The roughly cosine-shaped background as indicated by the dashed line in the figure is due to an admixture of the transverse Ettingshausen-Nernst voltage, analogous to the Hall voltage admixtures in the magnetoresistance.<sup>10</sup>

The field dependence of the thermopower for the magnetic field at one of the two peaks is shown in Fig. 3 (dots are measured values). The thermopower begins to oscillate for  $H > 10$  kG with a period  $\Delta(1/H) = 2.12 \times 10^{-6}$  G<sup>-1</sup>. The experimental data can be fitted by a single harmonic oscillation with exponential decay. The fit by the function

$$S = A e^{-H'/H} \sin(2F/H + \alpha) \quad (1)$$

with free parameters  $A$ ,  $H'$ ,  $F$ , and  $\alpha$  is given by the solid curve in Fig. 3. Similar measurements

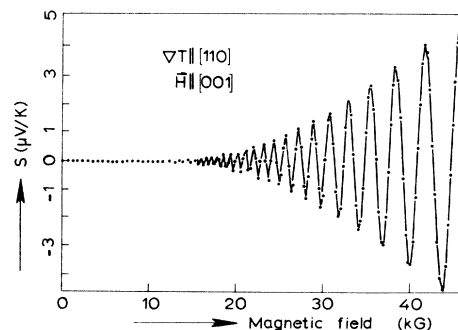


FIG. 3. Thermopower as function of the magnetic field  $\vec{H}$  at one of the two peaks of Fig. 2 (represented by dots) in comparison with the calculated (solid curve).

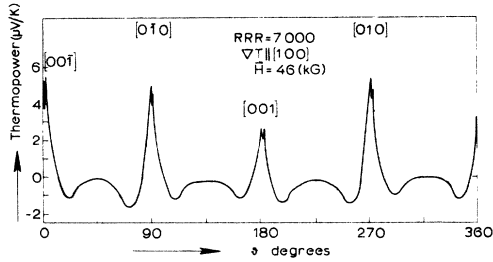


FIG. 4. Rotation diagram of the thermopower for  $\nabla T$  parallel to the  $[100]$  direction and  $H=46$  kG.

were also performed at different angles of rotation of the specimen. The parameters obtained from the corresponding fits are given in Table I. The large variation in  $A$  is reflected in the rotation diagram of Fig. 2.

#### B. (100) rotation plane

Figure 4 shows the thermopower of a sample in a constant magnetic field as a function of the rotation angle for  $\nabla T$  parallel to the  $[100]$  direction. The magnetic field intensity amounts to 46 kG and the residual resistivity ratio of the investigated sample was 7000. In this rotation diagram there occur four maxima for  $\vec{H}||[001]$  and  $[010]$ . These maxima show double peaks similar to those observed in the  $[110]$  oriented sample. The separation between the peaks amounts to about  $2^\circ$ . The orientation diagram of this specimen is in agreement with the thermopower measurements of Sirota *et al.*,<sup>3</sup> who used aluminum single crystals with a RRR of about 19 000.

The field dependence of the thermopower for an angle near one of the double peaks oscillates also with a period  $2.12 \times 10^{-6} \text{ G}^{-1}$ , which is in good agreement with dHVA,<sup>11</sup> with magnetoresistance,<sup>4,12</sup> and with hard helicon measurements,<sup>13</sup> but in dis-

TABLE I. Parameters defined in Eq. (1) for different angles.

Angle $\vartheta$	$A$ ( $\mu\text{V}/\text{K}$ )	$H'$ (kG)	$F$ (kG)	$\alpha$
$53^\circ$	42.3	97.4	466.3	$-68.7$
$57^\circ$	48.3	101.0	466.3	$-68.7$
$67^\circ$	15.15	107.5	463.1	$-70.5$
$88^\circ$	2.37	117.3	520.4	$-79.0$
$145^\circ$	0.155	80.3	509.3	$-84.0$

agreement with the measurements of Sirota *et al.*,<sup>3</sup> who found a period of  $1.877 \times 10^{-6} \text{ G}^{-1}$ .

#### C. (112) rotation plane

Figure 5(a) shows the rotation diagram of the thermopower for a sample with residual resistivity ratio of 4400 in a transverse magnetic field. The temperature gradient  $\nabla T$  was parallel to the  $[112]$  direction, while the field intensity was about 46.8 kG. A small peak occurs in the diagram for the orientation  $\vec{H}$  parallel to  $[1\bar{1}0]$ , which is equivalent to a pronounced peak in the rotation diagram of the magnetoresistance.<sup>4</sup> The cosine-shaped background is again due to an admixture of transverse Ettingshausen-Nernst voltage. The field dependence of the thermopower for the orientation  $\vec{H}$  parallel to  $[001]$  is shown in Fig. 5(b). Oscillations can be detected in the magnetothermopower, in contradiction to the magnetoresistance measurements for the same specimen.<sup>4</sup> The oscillations for this direction exist although their amplitude is smaller than that of the other directions. This is an indication that thermopower measurements are more sensitive than magnetoresistance and therefore more appropriate for studying magnetic breakdown effects.

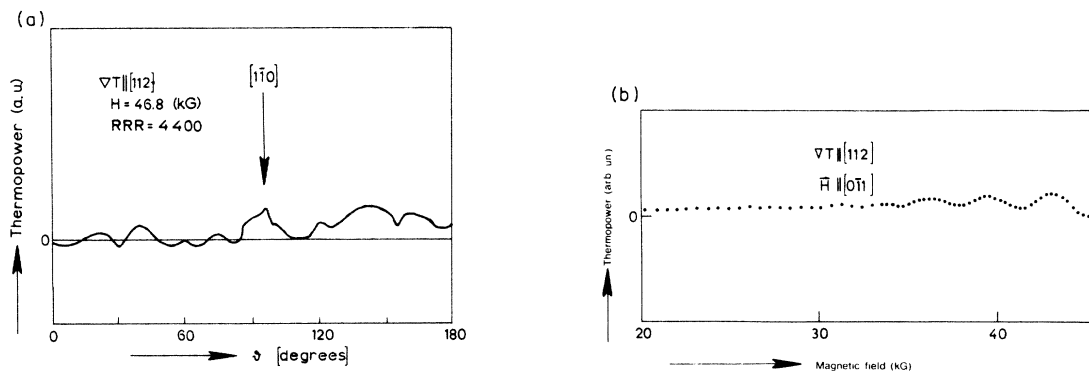


FIG. 5. (a) Rotation diagram of the thermopower for  $\nabla T$  parallel to  $[112]$  direction and at  $H=46.8$  kG; (b) Field dependence of the thermopower for  $\nabla T$  parallel to  $[112]$  and  $\vec{H}$  parallel to the  $[011]$  direction.

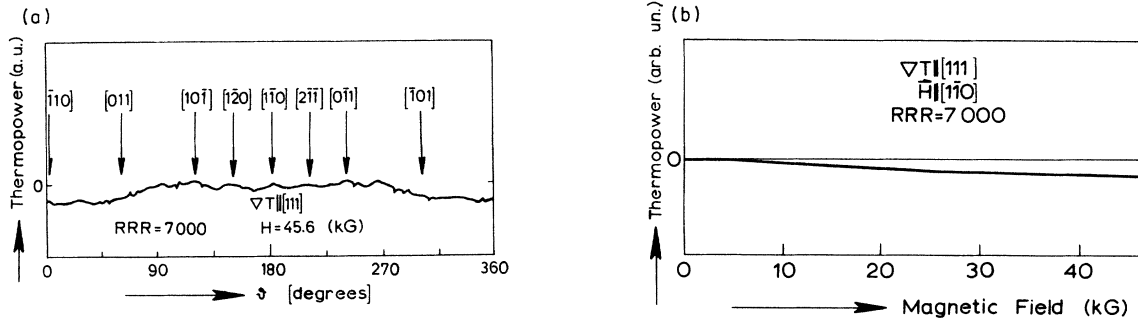


FIG. 6. (a) Rotation diagram of the magnetothermopower for  $\nabla T$  parallel to [111] and at  $H = 46.5$  kG; (b) Field dependence of the thermopower for  $\nabla T$  parallel to [111] and  $\vec{H}$  parallel to the [011] direction.

#### D. (111) rotation plane

In Fig. 6(a) is shown the rotation diagram of the thermopower of a sample with a  $RRR = 7000$  in a transverse magnetic field of  $46.5$  kG. The temperature gradient  $\nabla T$  was oriented parallel to the [111] direction. The diagram exhibits a very small anisotropy similar to the magnetoresistance measurements<sup>4</sup> and to the helicon measurements<sup>13</sup> and there are no peak regions. The field dependence of the thermopower for  $\vec{H}$  parallel to the [011] direction is shown in Fig. 6(b), in which no oscillatory component was detected, as in the magnetoresistance.

#### E. Ettingshausen-Nernst effect

Figure 7(a) shows the rotation diagram of the transverse Ettingshausen-Nernst voltage for  $\nabla T$  parallel to the [100] direction and in a constant magnetic field of  $48.5$  kG. The Ettingshausen-Nernst voltage has a cosine shape and, for  $\vec{H}$  parallel to the [100] direction, develops a minimum and a maximum which correspond to the double maximum in the thermopower.

The magnetic field dependence of the Ettings-

hausen-Nernst voltage at the maximum of the rotation diagram is shown in Fig. 7(b). This voltage shows a purely oscillatory behavior same as the thermopower. The oscillations again are periodic in  $1/H$ , exhibiting only a single harmonic with a period of  $2.12 \times 10^{-6} \text{ G}^{-1}$ . This agrees with the value obtained by the thermopower and it is attributed to phase coherence around the  $\beta$  orbit. The relative magnitude of the oscillations in the Ettingshausen-Nernst effect compared to that in the thermopower is about 1 to 8. It must be emphasized that in contradiction to the Ettingshausen-Nernst voltage no oscillations are observed in the Hall coefficient of the same sample.

#### IV. DISCUSSION

Because the oscillations in the magnetothermopower occur in a small angular region only, we infer that these oscillations do not result from quantized Landau levels or, equivalently, from quantized closed orbits, but rather result from magnetic breakdown. The magnetic breakdown probability oscillates as a function of magnetic field  $H$  due to the requirement of phase coherence of the

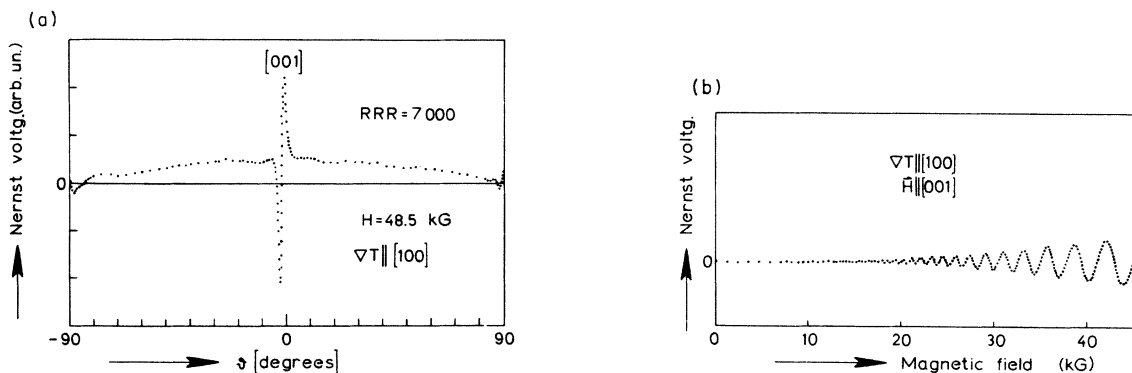


FIG. 7. (a) Rotation diagram of Ettingshausen-Nernst voltage for  $\nabla T$  parallel to the [100] direction and at  $H = 48.5$  kG; (b) Field dependence of Ettingshausen-Nernst voltage at the maximum of the rotation diagram.

wave function in the involved orbits. Because of the phase smearing,<sup>14</sup> only the oscillations from the third zone are visible in our experiments. The period of the oscillations leads according to Onsager's relation<sup>15</sup> to an area of  $(4.505 \times 10^{-3}) \text{ \AA}^{-2}$  which for a rotation angle of about  $55^\circ$  corresponds to the  $\beta$  orbit in the third zone Fermi surface. The values for  $F$  in Table I show that rotation to other values of angle  $\vartheta$  does not significantly change the area of the orbit involved in magnetic breakdown, although the plane of the orbit moves around the elbow of the third zone Fermi surface arm when  $\vartheta$  is changed from  $55^\circ$  to  $145^\circ$ . Also  $\alpha$  and  $H'$  do not change significantly with  $\vartheta$ . The meaning of  $\alpha$  is not understood, while  $H'$  is mainly determined by the breakdown field  $H_0$  as discussed in the following. On the other hand, the amplitude  $A$  decreases rapidly as we rotate the sample from  $55^\circ$  to  $145^\circ$ , due to the decreasing probability of satisfying the "double junction" criterion, as required for transition of a closed orbit into an open one, as discussed in Ref. 4.

The probability of magnetic breakdown increases towards higher magnetic fields as  $\exp(-H_0/H)$  where  $H_0$  is the breakdown field. On the other hand, electronic scattering due to lattice imperfections and finite temperature also lead to magnetic-field-dependent amplitudes. From the treatment by Dingle<sup>16</sup> of these scattering-dependent terms, we obtain for our case of a single harmonic oscillation and for not too high magnetic fields another exponential term in  $1/H$ ,  $\exp[-2\pi^2 k_B(T+T^D)/\hbar\omega_c]$  where  $T^D = \hbar/2\pi k_B \tau$ ,  $\tau$  the relaxation time between scattering events at lattice imperfections and  $\omega_c = eH/m_c c$ ,  $m_c$  the cyclotron mass. Inserting this into the empirical formula (1) yields for the parameter  $H'$

$$H' = H_0 + (2\pi^2 m_c c/e) k_B (T + T^D).$$

We assume that in our carefully prepared single crystals the Dingle temperature  $T^D$  due to impurity and dislocation scattering does not exceed  $4^\circ$ . For the experimental values  $H'$  the breakdown field can be calculated,  $H_0 = 70 \pm 10$  kG.

To explain the close relationship between the magnetic breakdown effects which we observed in the magnetoresistance and in the thermopower we try to extend the Mott relation between electrical conductivity  $\sigma$  and thermopower  $S$  to the case of magnetic breakdown.

$$S(H) = \frac{\pi^2}{3} \frac{k_B}{e} k_B T \left( \frac{\partial \ln \sigma(H)}{\partial \epsilon} \right)_{\epsilon = \epsilon_F}, \quad (2)$$

where  $k_B$ ,  $e$ ,  $T$ , and  $\epsilon_F$  are the Boltzmann constant, electronic charge, the temperature, and the Fermi energy, respectively. Equation (2) reduces to the relation

$$S(H) = \frac{\pi^2}{3} \frac{k_B}{e} k_B T \frac{1}{\sigma(H)} \left( \frac{\partial \sigma(H)}{\partial \epsilon} \right)_{\epsilon = \epsilon_F}. \quad (3)$$

From our measurements of the magnetoresistance<sup>4</sup> we can deduce that the electrical conductivity can be written as a sum of a monotonic part and an oscillatory part. The latter is due to the few orbits which undergo magnetic breakdown from closed into open orbits. Our data may be fitted by an equation of the form

$$\sigma(H) = A_0(H) + A_1 e^{-H'/H} \sin(2\pi F/H + \alpha_1), \quad (4)$$

which is similar to Eq. (1) for the thermopower with additional free parameters  $A_1$  and  $\alpha_1$ . As we have shown,  $H'$  is the sum of electron scattering term and the breakdown field  $H_0 = (\Delta\epsilon)^2 H / \hbar\omega_c \epsilon_F$ .  $\omega_c$  is the cyclotron frequency, and  $\Delta\epsilon$  is the energy gap between the bands at the point at which magnetic breakdown occurs.

In Eq. (3), the term  $\sigma(H)$  becomes  $A_0(H)$ , because the oscillatory part is very small due to the fact that  $H_0 \gg H$ . However, in the derivative,  $[\partial \sigma(H)/\partial \epsilon]_{\epsilon_F}$ , the oscillatory term predominates, so that

$$\frac{1}{\sigma(H)} \frac{\partial \sigma}{\partial \epsilon} \Big|_{\epsilon = \epsilon_F} = - \frac{2\Delta\epsilon}{\hbar\omega_c \epsilon_F} \frac{\sigma_{\text{osc}}}{\sigma} = - \frac{2H_0}{\Delta\epsilon H} \frac{\sigma_{\text{osc}}}{\sigma}.$$

So, the thermopower oscillates in a magnetic field with the same frequency  $F$  as the electrical conductivity, namely,

$$S(H) = - \frac{2\pi^2}{3} \frac{k_B}{e} \frac{k_B T}{\Delta\epsilon} \frac{H_0}{H} \frac{\sigma_{\text{osc}}}{\sigma}. \quad (5)$$

Thus, it is the sensitivity of magnetic breakdown to changes in energy that makes the thermovoltage so sensitive to magnetic breakdown effects. Using our magnetoresistance data for  $\sigma_{\text{osc}}/\sigma$  we can estimate the voltage of  $S$  in Eq. (5). At 40 kG a value of about  $1 \mu\text{V/K}$  is obtained which has the right order of magnitude.

In our previous magnetoresistance measurements<sup>4</sup> we have discussed in detail the network of coupled orbits in aluminum between the second and third zone, which occur due to magnetic breakdown near the  $W$  point of the Brillouin zone.

In order to consider what types of extended orbits are, we used the so called "double junction" criterion. Because of the similarity of the experimental results for magnetoresistivity and thermopower in aluminum, the same networks of coupled orbits can be considered to explain the rotation diagrams of the thermopower, namely: (a) If the temperature gradient  $\nabla T$  is parallel to the [001] direction, open orbits occur for all directions of magnetic field  $\vec{H}$  except for  $\vec{H}$  parallel to [100], which is a singular direction. For this direction we do not have open orbits and the magnetothermo-

power shows a relative minimum. (b) For the case that  $\nabla T$  is parallel to the  $[011]$  direction, the double peak which occurs at  $\vec{H}$  parallel to  $[100]$  originates for the same reasons as in case (a). (c) For  $\nabla T$  parallel to  $[112]$  and  $\vec{H}$  parallel to  $[111]$ , open orbits are created for  $\vec{H}$  parallel to  $[1\bar{1}0]$ , giving rise to the single peaks at  $\vec{H}$  parallel to  $[1\bar{1}0]$ .

#### V. CONCLUSION

We have measured the orientation diagrams and the field dependence of the transverse magnetothermopower and Ettingshausen-Nernst voltage of a series of single-crystal aluminum samples with different orientations. The orientation diagrams

of the thermopower show similar behavior to those of the magnetoresistance, and their field dependences oscillate with the same period as the magnetoresistance. Because of the similarity between magnetothermopower and magnetoresistivity in aluminum, we have concluded that the same networks of orbits occur as discussed in previous measurements on the magnetoresistivity.

#### ACKNOWLEDGMENT

We would like to thank Professor Jack Bass of Michigan State University for reading the manuscript and in particular for his useful comments and suggestions.

<sup>1</sup>W. Kesternich and C. Papastaikoudis, *Phys. Status Solidi* **46**, K41 (1974).

<sup>2</sup>B. J. Thaler and J. Bass, *J. Phys. F* **5**, 1554 (1975).

<sup>3</sup>N. N. Sirota, V. I. Gostishev, and A. A. Drozd, *Dokl. Akad. Nauk SSSR* **220**, 818 (1975) [*Sov. Phys. Dokl.* **20**, 2116 (1975)].

<sup>4</sup>W. Kesternich and C. Papastaikoudis, *J. Phys. F* **7**, 837 (1977).

<sup>5</sup>J. W. Ekin and B. W. Maxfield, *Phys. Rev. B* **2**, 4805 (1970).

<sup>6</sup>A. R. De Vroomen, C. van Baarle, and A. J. Cuelenaere, *Physica (Utr.)* **26**, 19 (1960).

<sup>7</sup>I. Holwech and V. Sollin, *Phys. Status Solidi* **34**, 403 (1969).

<sup>8</sup>R. S. Averback and D. K. Wagner, *Solid State Com-*

*mun.* **11**, 1109 (1973).

<sup>9</sup>R. S. Averback, C. H. Stephan, and J. Bass, *J. Low Temp. Phys.* **12**, 319 (1973).

<sup>10</sup>W. Kesternich, H. Ullmaier, and W. Schilling, *Philos. Mag.* **31**, 471 (1975).

<sup>11</sup>C. O. Larson and W. L. Gordon, *Phys. Rev.* **156**, 703 (1967).

<sup>12</sup>R. C. Balcombe and R. A. Parker, *Philos. Mag.* **21**, 533 (1970).

<sup>13</sup>J. A. Delaney, *J. Phys. F* **4**, 247 (1974).

<sup>14</sup>R. C. Young, *J. Phys. F* **3**, 721 (1973).

<sup>15</sup>J. M. Ziman, *Principles of the Theory of Solids* (Cambridge U.P., Cambridge, 1964), pp.194-196.

<sup>16</sup>R. B. Dingle, *Proc. R. Soc. A* **311**, 517 (1952).